molecular pharmaceutics

articles

The Mechanism of Polyplex Internalization into Cells: Testing the GM1/Caveolin-1 Lipid Raft Mediated Endocytosis Pathway

Rong Qi,*[,†,‡,§,∥] Douglas G. Mullen,[∥,⊥] James R. Baker, Jr.,[∥] and Mark M. Banaszak Holl*[,§,∥,⊥]

Peking University Institute of Cardiovascular Sciences, Peking University Health Science Center, Peking University, Beijing 100083, China, Key Laboratory of Molecular Cardiovascular Sciences, Ministry of Education, China, and Chemistry Department, Program in Macromolecular Science and Engineering, and the Michigan Nanotechnology Institute for Medicine and Biological Sciences, University of Michigan, Ann Arbor, Michigan 48109-1055

Received September 23, 2009; Revised Manuscript Received December 15, 2009; Accepted December 21, 2009

Abstract: The GM1/caveolin-1 lipid raft mediated endocytosis mechanism was explored for generation 5 and 7 poly(amidoamine) dendrimer polyplexes employing the Cos-7, 293A, C6, HeLa, KB, and HepG2 cell lines. Expression levels of GM1 and caveolin-1 were measured using dot blot and Western blot, respectively. The level of GM1 in the cell plasma membrane was adjusted by incubation with exogenous GM1 or ganglioside inhibitor PPMP, and the level of CAV-1 was adjusted by upregulation with the adenovirus vector expressed caveolin-1 (AdCav-1). Cholera toxin B subunit was employed as a positive control for uptake in all cases. No evidence was found for a GM1/caveolin-1 lipid raft mediated endocytosis mechanism for the generation 5 and 7 poly(amidoamine) dendrimer polyplexes.

Keywords: PAMAM dendrimer; polyplexes; endocytosis; transfection; ganglioside GM1; caveolin-1

Poly(amidoamine) PAMAM dendrimers show exceptional promise as drug delivery vehicles and have proven to be effective vectors for cell transfection.[1,2] Both Middaugh et al. and Baker et al. studied transfection and expression as a function of dendrimer generation.[3−6] Szoka et al. demonstrated that the transfection efficiency of PAMAM dendrimer-based polyplexes could be dramatically enhanced by heating

* Corresponding authors. Mailing address: University of Michigan, Department of Chemistry, 930 N. University Ave., Ann Arbor, MI 48109-1055. Tel: 734-763-2283. Fax: 734-763-2283. E-mail: mbanasza@umich.edu.

† Peking University.

‡ Ministry of Education, China.

§ Chemistry Department, University of Michigan.

∥ Michigan Nanotechnology Institute for Medicine and Biological Sciences, University of Michigan.

⊥ Program in Macromolecular Science and Engineering, University of Michigan.

(1) Lee, C. C.; MacKay, J. A.; Frechet, J. M. J.; Szoka, F. C. Designing dendrimers for biological applications. *Nat. Biotechnol.* **2005**, *23*, 1517–1526.

(2) Eichman, J. D.; Bielinska, A. U.; Kukowska-Latallo, J. F.; Donovan, B. W.; Baker, J. R., Bioapplications of PAMAM Dendrimers. In *Dendrimers and Other Dendritic Polymers*; Frechet, J. M. J., Tomalia, D. A., Eds.; John Wiley & Sons: New York, 2001; pp 441−461.

(3) Braun, C. S.; Fisher, M. T.; Tomalia, D. A.; Koe, G. S.; Koe, J. G.; Middaugh, C. R. A stopped-flow kinetic study of the assembly of nonviral gene delivery complexes. *Biophys. J.* **2005**, *88*, 4146–4158.

(4) Braun, C. S.; Vetro, J. A.; Tomalia, D. A.; Koe, G. S.; Koe, J. G.; Middaugh, C. R. Structure/function relationships of poly(amidoamine)/DNA dendrimers as gene delivery vehicles. *J. Pharm. Sci.* **2005**, *94*, 423–436.

(5) Kukowska-Latallo, J. F.; Bielinska, A. U.; Johnson, J.; Spindler, R.; Tomalia, D. A.; Baker, J. R. Efficient transfer of genetic material into mammalian cells using Starburst polyamidoamine dendrimers. *Proc. Natl. Acad. Sci. U.S.A.* **1996**, *93*, 4897–4902.

10.1021/mp900241t
Published on Web 12/21/2009

the dendrimer in water or butanol.[7,8] These "fractured" dendrimers form the basis of the highly successful commercial transfection reagent SuperFect (Qiagen). When PAMAM dendrimer/DNA polyplexes are employed for cell transfection, the dendrimers are mixed with the desired oligonucelotide paying close attention to the ratio between the number of primary amines on the dendrimer (*N*) and the number of phosphates on the DNA (*P*). The *N*/*P* ratio indicates the net charge on the resulting polyplex and needs to have a value >1 for effective interaction with the cell membrane and internalization of the polyplex into the cell. Because of their regular branched structure and well-controlled polydispersity, PAMAM dendrimers provide an excellent experimental system for forming polyplexes with a well-controlled *N*/*P* ratio. For these reasons, PAMAM dendrimer-based cationic polyplexes also serve as good model system for exploring polyplexes binding and uptake mechanisms into cells as part of the transfection process.

The mechanism(s) of cationic polyplex cellular internalization have been intensely studied.[9−11] A variety of cationic polymers have been employed in these studies including PAMAM dendrimers,[12,13] poly(ethyleneimine) (PEI),[14−17] and poly-L-lysine (PLL).[18] For PAMAM/DNA polyplexes, George et al. presented evidence supporting a lipid raft mediated endocytosis (LRME) process based upon colocalization with cholera toxin subunit B (CTB) and a decreased transfection efficiency upon preincubation with methyl-β-cyclodextrin (Mβ-CD).[12] In subsequent work, they also noted that overexpression of caveolin-1 enhanced uptake and transfection efficiency.[13] Many other studies have been performed on the uptake mechanism of cationic dendrimers themselves without DNA present.[19−26] However, the relevance of the dendrimers only mechanistic studies to understanding the uptake of polyplexes is unclear because of the substantial size difference between the individual dendrimers (3−10 nm)[27] and the dendrimer/DNA polyplexes (~100−400 nm).[3,4] Numerous studies have demonstrated that particle size affects both uptake and transfection efficiency.[28−30]

An alternative mechanism for the uptake of cationic polyplexes has been proposed involving interaction with the cell plasma membrane proteoglycans. Baldeschwieler et al.

(6) Kukowska-Latallo, J. F.; Raczka, E.; Quintana, A.; Chen, C. L.; Rymaszewski, M.; Baker, J. R. Intravascular and endobronchial DNA delivery to murine lung tissue using a novel, nonviral vector. *Hum. Gene Ther.* **2000**, *11*, 1385–1395.

(7) Tang, M. X.; Redemann, C. T.; Szoka, F. C. In vitro gene delivery by degraded polyamidoamine dendrimers. *Bioconjugate Chem.* **1996**, *7*, 703–714.

(8) Tang, M. X.; Szoka, F. C. The influence of polymer structure on the interactions of cationic polymers with DNA and morphology of the resulting complexes. *Gene Ther.* **1997**, *4*, 823–832.

(9) Behr, J. P. Synthetic Gene-Transfer Vectors. *Acc. Chem. Res.* **1993**, *26*, 274–278.

(10) Behr, J. P. The proton sponge: A trick to enter cells the viruses did not exploit. *Chimia* **1997**, *51*, 34–36.

(11) Mintzer, M. A.; Simanek, E. E. Nonviral Vectors for Gene Delivery. *Chem. Rev.* **2009**, *109*, 259–302.

(12) Manunta, M.; Tan, P. H.; Sagoo, P.; Kashefi, K.; George, A. J. T. Gene delivery by dendrimers operates via a cholesterol dependent pathway. *Nucleic Acids Res.* **2004**, *32*, 2730–2739.

(13) Manunta, M.; Nichols, B. J.; Tan, P. H.; Sagoo, P.; Harper, J.; George, A. J. T. Gene delivery by dendrimers operates via different pathways in different cells, but is enhanced by the presence of caveolin. *J. Immunol. Methods* **2006**, *314*, 134–146.

(14) Boussif, O.; Lezoualch, F.; Zanta, M. A.; Mergny, M. D.; Scherman, D.; Demeneix, B.; Behr, J. P. A Versatile Vector for Gene and Oligonucleotide Transfer into Cells in Culture and in-Vivo—Polyethylenimine. *Proc. Natl. Acad. Sci. U. S. A.* **1995**, *92*, 7297–7301.

(15) Kopatz, I.; Remy, J. S.; Behr, J. P. A model for non-viral gene delivery: through syndecan adhesion molecules and powered by actin. *J. Gene Med.* **2004**, *6*, 769–776.

(16) Erbacher, P.; Remy, J. S.; Behr, J. P. Gene transfer with synthetic virus-like particles via the integrin-mediated endocytosis pathway. *Gene Ther.* **1999**, *6*, 138–145.

(17) Boeckle, S.; von Gersdorff, K.; van der Piepen, S.; Culmsee, C.; Wagner, E.; Ogris, M. Purification of polyethylenimine polyplexes highlights the role of free polycations in gene transfer. *J. Gene Med.* **2004**, *6*, 1102–1111.

(18) Mislick, K. A.; Baldeschwieler, J. D. Evidence for the role of proteoglycans in cation-mediated gene transfer. *Proc. Natl. Acad. Sci. U.S.A.* **1996**, *93*, 12349–12354.

(19) Perumal, O. P.; Inapagolla, R.; Kannan, S.; Kannan, R. M. The effect of surface functionality on cellular trafficking of dendrimers. *Biomaterials* **2008**, *29*, 3469–3476.

(20) Kitchens, K. M.; Kolhatkar, R. B.; Swaan, P. W.; Ghandehari, H. Endocytosis inhibitors prevent poly(amidoamine) dendrimer internalization and permeability across Caco-2 cells. *Mol. Pharmaceutics* **2008**, *5*, 364–369.

(21) Jevprasesphant, R.; Penny, J.; Attwood, D.; McKeown, N. B.; D'Emanuele, A. Engineering of dendrimer surfaces to enhance transepithelial transport and reduce cytotoxicity. *Pharm. Res.* **2003**, *20*, 1543–1550.

(22) Seib, F. P.; Jones, A. T.; Duncan, R. Comparison of the endocytic properties of linear and branched PEIs, and cationic PAMAM dendrimers in B16f10 melanoma cells. *J. Controlled Release* **2007**, *117*, 291–300.

(23) Hong, S.; Bielinska, A. U.; Mecke, A.; Keszler, B.; Beals, J. L.; Shi, X.; Balogh, L.; Orr, B. G.; Baker, J. R.; Banaszak Holl, M. M. The Interaction of Poly(amidoamine) (PAMAM) Dendrimers with Supported Lipid Bilayers and Cells: Hole Formation and the Relation to Transport. *Bioconjugate Chem.* **2004**, *15*, 774–782.

(24) Hong, S.; Leroueil, P. R.; Janus, E. K.; Peters, J. L.; Kober, M. M.; Islam, M. T.; Orr, B. G.; Baker, J. R.; Holl, M. M. B. Interaction of polycationic polymers with supported lipid bilayers and cells: Nanoscale hole formation and enhanced membrane permeability. *Bioconjugate Chem.* **2006**, *17*, 728–734.

(25) Leroueil, P. R.; Hong, S.; Mecke, A.; Baker, J. R.; Orr, B. G.; Holl, M. M. B. Nanoparticle interaction with biological membranes: Does nanotechnology present a Janus face. *Acc. Chem. Res.* **2007**, *40*, 335–342.

(26) Hong, S.; Rattan, R.; Majoros, I.; Mullen, D. G.; Peters, J. L.; Shi, X.; Bielinska, A. U.; Blanco, L.; Orr, B. G.; Baker, J. R.; Banaszak Holl, M. M. The Role of Ganglioside GM_1 in Cellular Internalizatino Mechanisms of Poly(amidoamine) Dendrimers. *Bioconjugate Chem.* **2009**, *20*, 1503–1513.

(27) Li, J.; Peihler, L. T.; Qin, D.; Baker, J. R.; Tomalia, D.; Meier, D. Visualization and Characterization of Poly(amidoamine) Dendrimers by Atomic Force Microscopy. *Langmuir* **2000**, *16*, 5613–5616.

demonstrated this dependence for PLL/DNA polyplexes,[18] and Debs et al. demonstrated this for cationic liposome/DNA polyplexes.[31] Further studies by Behr et al. indicated an initial interaction with heparan sulfate proteoglcyans (syndecans) triggering an actin-mediated endocytosis event.[15] To date, no studies have tested these hypotheses for dendrimer-based polyplexes.

In designing this study of PAMAM/DNA polyplex uptake, we decided to test the hypothesis that cellular uptake was a GM1/caveolin-1 mediated LRME process (GM1 = monosialotetrahexosylganglioside). We focused on testing this pathway for the following reasons: (1) The CTB colocalization data were a particularly compelling piece of evidence supporting a GM1-based internalization pathway. (2) Data supporting a role for caveolin-1 has also been obtained thus providing a consistent picture of a LRME pathway. (3) Colocalization with CTB and caveolin-1 (CAV-1) dependence had also been observed for PEI/DNA polyplexes.[32] (4) Evidence indicating that polyplexes internalized via caveolae escape the lysosome, thus permitting efficient transfection, has also been presented for PEI/DNA polyplexes.[33] Despite the compelling nature of this evidence, additional studies to test the mechanistic hypothesis are important. For the study presented here, the involvement of GM1 is probed by employing the C6 cell and quantifying GM1 using horseradish peroxidase (HRP) labeled CTB in dot blot. We also employed a general ganglioside inhibitor DL-threo-1-phenyl-2-palmitoylamino-3-morpholino-1-propanol (PPMP) to block the synthesis of GM1.[34] Lastly, we explored the role of CAV-1 following expression level across cell types, including viral upregulation. For these studies, C6 cells were employed because they are GM1 deficient but CAV-1 sufficient. Cos-7 and 293A cells were employed because they are sufficient in both GM1 and CAV-1. HeLa, KB, and HepG2 cells were employed because they are doubly deficient, to different degrees, in both GM1 and CAV-1. The results of these studies indicate that the GM1/caveolin-1 mediated LRME pathway is not followed for Cos-7, 293A, C6, HeLa, KB, or HepG2 cell lines.

This work is most relevant for understanding the in vitro transfection process, since serum was avoided in the formation and transfection of polyplexes to minimize the degradation of DNA and polyplexes by DNases and negatively charged proteins, respectively.[35−37] When considering the relevance to the in vivo mechanism of polyplexes it should be kept in mind that the serum proteins are not present.

Materials

G7 and G5 PAMAM dendrimers were purchased from Dendritech Inc. (Midland, MI) and purified before use. Alexa Fluor 488 carboxylated, succinimidyl ester (AF488), recombinant cholera toxin subunit B-Alexa Fluor 647 conjugate (CTB-AF647) and horseradish peroxidase conjugate (CTB-HRP) were supplied by Molecular Probes (Eugene, OR). Monosialoganglioside GM1 (NH_4^+ salt) and DL-threo-1-phenyl-2-palmitoylamino-3-morpholino-1-propanol (PPMP) were provided by Matreya (Pleasant Gap, PA). LabelIt tracker Cy5 intracellular nucleic acid localization kit was obtained from Mirus Bio Corporation (Madison, WI). Mouse anti-α-tubulin antibody and goat anti-mouse IgG were provided by Sigma-Aldrich (St. Louis, MO). Rabbit anti-caveolin-1 polyclonal antibody (N-20), goat anti-rabbit IgG-HRP and IgG-TRITC were purchased from Santa Cruz (Santa Cruz, CA). Ad-Caveolin-1 and Ad-CMV-Null were from Vector Biolabs (Philadelphia, PA). BCA protein assay kit was ordered from Pierce Inc. (Rockford, IL). SuperSignal West Pico Chemiluminescent Substrate (HRP detection kit) was from Thermo Scientific (Rockford, IL). All other chemicals were acquired from Aldrich and used as received.

Methods

AF488 Labeled G5 and G7 Amine Dendrimers. To remove the lower molecular weight impurities and trailing generations from the purchased products, generation 5 and 7 PAMAM dendrimers (G5-NH_2, G7-NH_2) were dialyzed against a 10,000 (for G5) or 50,000 (for G7) molecular weight cutoff (MWCO) membrane with DI water for three

(28) Xu, D. M.; Yao, S. D.; Liu, Y. B.; Sheng, K. L.; Hong, J.; Gong, P. J.; Dong, L. Size-dependent properties of M-PEIs nanogels for gene delivery in cancer cells. *Int. J. Pharm.* **2007**, *338*, 291–296.

(29) Prabha, S.; Zhou, W. Z.; Panyam, J.; Labhasetwar, V. Size-dependency of nanoparticle-mediated gene transfection: studies with fractionated nanoparticles. *Int. J. Pharm.* **2002**, *244*, 105–115.

(30) Desai, M. P.; Labhasetwar, V.; Walter, E.; Levy, R. J.; Amidon, G. L. The mechanism of uptake of biodegradable microparticles in Caco-2 cells is size dependent. *Pharm. Res.* **1997**, *14*, 1568–1573.

(31) Mounkes, L. C.; Zhong, W.; Cipres-Palacin, G.; Heath, T. D.; Debs, R. J. Proteoglycans mediate cationic Liposome-DNA complex-based gene delivery in vitro and in vivo. *J. Biol. Chem.* **1998**, *273*, 26164–26170.

(32) van der Aa, M.; Huth, U. S.; Hafele, S. Y.; Schubert, R.; Oosting, R. S.; Mastrobattista, E.; Hennink, W. E.; Peschka-Suss, R.; Koning, G. A.; Crommelin, D. J. A. Cellular uptake of cationic polymer-DNA complexes via caveolae plays a pivotal role in gene transfection in COS-7 cells. *Pharm. Res.* **2007**, *24*, 1590–1598.

(33) Rejman, J.; Bragonzi, A.; Conese, M. Role of clathrin- and caveolae-mediated endocytosis in gene transfer mediated by lipo- and polyplexes. *Mol. Ther.* **2005**, *12*, 468–474.

(34) Masson, E.; Wiernsperger, N.; Lagarde, M.; El Bawab, S. Involvement of gangliosides in glucosamine-induced proliferation decrease of retinal pericytes. *Glycobiology* **2005**, *15*, 585–591.

(35) Chonco, L.; Bermejo-Martin, J. F.; Ortega, P.; Shcharbin, D.; Pedziwiatr, E.; Klajnert, B.; de la Mata, F. J.; Eritja, R.; Gomez, R.; Bryszewska, M.; Munoz-Fernandez, M. A. Water-soluble carbosilane dendrimers protect phosphorothioate oligonucleotides from binding to serum proteins. *Org. Biomol. Chem.* **2007**, *5*, 1886–1893.

(36) Klajnert, B.; Stanislawska, L.; Bryszewska, M.; Palecz, B. Interactions between PAMAM dendrimers and bovine serum albumin. *Biochim. Biophys. Acta* **2003**, *1648*, 115–126.

(37) Urtti, A.; Polansky, J.; Lui, G. M.; Szoka, F. C. Gene delivery and expression in human retinal pigment epithelial cells: Effects of synthetic carriers, serum, extracellular matrix and viral promoters. *J. Drug Targeting* **2000**, *7*, 413–421.

days, exchanging washes every 4 h. The average molecular weight (27,336 g/mol for G5, 113,800 g/mol for G7) and polydispersity index (PDI) of the G5 (1.02) and G7 (1.11) dendrimers were determined by gel permeation chromatography (GPC). Potentiometric titration was conducted to determine the average number of primary amines per dendrimer on G5 (112) and G7 (475).

To label the dendrimer with fluorescence, the purified G5-NH_2 dendrimer (0.0250 g, 0.915 μmol) was dissolved in 1× PBS (5.8 mL). Alexa Fluor 488 (0.0029 g, 4.6 μmol) was dissolved in 1.5 mL of DMSO and added in a dropwise fashion to the dendrimer solution. The resulting mixture was stirred for 4 days at room temperature under nitrogen. The reaction mixture was then purified by size exclusion chromatography using Sephadex G-25 beads in 1× PBS. The dendrimer fraction was collected, and the elution buffer was exchanged with deionized (DI) water using 10,000 MWCO Amicon Ultra centrifugal filtration devices (three cycles of 10 min at 5,000 rpm). The purified product was lyophilized to yield an orange solid (25.3 mg, 95%). ^{1}H NMR integration determined an average of 2.6 Alexa Fluor 488 molecules coupled to the dendrimer. HPLC was used to determine that all unreacted dye molecules were successfully removed by purification.

The procedure used to label the purified G7-NH_2 dendrimer with Alexa Fluor 488 was identical to that of the G5-NH_2 dendrimer with the following changes: G7-NH_2 dendrimer (0.0338 g, 0.297 μmol) was dissolved in 1× PBS (2.039 mL). Alexa Fluor 488 (0.0011 g, 1.6 μmol) was dissolved in 0.535 mL of DMSO. The yield of the purified product was 33.7 mg (98%). ^{1}H NMR integration determined an average of 3.0 Alexa Fluor 488 molecules coupled to the dendrimer.

Cell Lines. The KB, HeLa, Cos-7, 293A, HepG2 and C6 cell lines were purchased from the American Type Culture Collection (ATCC, Manassas, VA) and grown continuously as a monolayer at 37 °C, and 5% CO_2. The KB cells were grown in RPMI 1640 medium (Mediatech, Herndon, VA). The Cos-7, HepG2 and 293A cells were grown in Dulbecco's modified Eagle's medium (DMEM, Gibco, Eggenstein, Germany). The HeLa and C6 cells were grown in F-12 Kaighn's medium (F-12K, Invitrogen, Carlsbad, CA). The RPMI 1640, DMEM and F-12K medium were supplemented with penicillin (100 units/mL), streptomycin (100 μg/mL), and 10% heat-inactivated fetal bovine calf serum (FBS) to make a complete medium before use. Rat glioma C6 cells were employed because they are GM1 deficient but CAV-1 sufficient. Fibroblast Cos-7 and epithelial 293A cells were employed because they are sufficient in both GM1 and CAV-1. Epithelial HeLa (cervix carcinoma) and KB (HeLa contaminant) and HepG2 (hepatoma) cells were employed because they are doubly deficient, to different degrees, in both GM1 and CAV-1.

Plasmid Amplification. To amplify the plasmid DNA, plasmid encoding luciferase and plasmid encoding green fluorescence protein (pGFP) (Clontech Laboratories, Inc., Mountain View, CA) were proliferated first in *Escherichia coli* and then purified by using QIAGEN plasmid purification kits. The plasmids obtained were identified by restriction enzymes, and DNA concentration was determined by UV spectrophotometry.

Cy5-Labeled Plasmid. A LabelIt tracker Cy5 kit was used to label the Luciferase plasmid according to the recommended protocol. Briefly, plasmid DNA was mixed with the tracker reagent at a ratio of 0.25 (v/w) (Cy5 reagent/DNA = 50 μL/200 μg) and incubated at 37 °C for 1 h. The labeled DNA was diluted by cold 5 M NaCl and 100% ethanol and then held at −20 °C for 2 h. The precipitated DNA was collected by centrifugation and rinsed with 70% ethanol. The DNA pellets were then redissolved in the desired volume of Tris-EDTA buffer. UV spectrophotometry was used to determine the concentration of plasmid DNA.

Formation of Polyplexes. To form polyplexes, equal volumes of plasmid solution (with 2 μg of DNA) and dendrimer solution were mixed in water at an *N*/*P* ratio of 10. The resulting mixture was incubated for 30 min at room temperature (RT) to form polyplexes. The particle size of polyplexes (100−500 nm, data not shown) was determined by dynamic light scattering (DLS).

The polyplexes formed by pGFP with G5 or G7 dendrimers were used in transfection experiments to detect transfection efficiency; the polyplexes made by Cy5-labeled plasmid Luciferase and AF488-labeled G5 or G7 dendrimers were employed in flow cytometry and confocal studies to explore the endocytosis mechanism of polyplexes. For transfection and endocytosis, the final concentration of dendrimer exposed to the cells was controlled to 4.3 μg/mL (157.3 nM G5-NH_2 or 37.7 nM G7-NH_2), which is the nontoxic concentration of dendrimers to the cells determined previously by XTT and LDH assay.[26]

Transfections. The cells were seeded on 24-well plates at a cell density of $4-5 \times 10^4$ cells per well in complete medium 24 h before transfection. Polyplexes were added to the cells (at 70−80% confluence, transfected in 400 μL of serum-free medium), and incubated for 3 h. The cells were rinsed with a serum-free medium and incubated with 500 μL of complete medium for 48 h. The fluorescence of GFP expressed in transfected cells was observed by fluorescence microscopy.

Endocytosis of Polyplexes. The cells were seeded on 6-well plates at a cell density of 2×10^5 cells per well in complete medium and grew to achieve a 70−80% confluence. Polyplexes made by fluorescence-labeled dendrimers and plasmid were added to the cells After being incubated for 3 h, the cells were rinsed with a serum-free medium and incubated with a complete medium for 3 h. The cells were then washed with PBS and fixed with 2% paraformaldehyde (PFA).

The fluorescence intensity of polyplexes associated with the cells or internalized inside the cells was measured by flow cytometry (BD Biosciences FACSCanto II, San Jose, CA). Voltages were set based upon the negative control and single fluorescence-stained cells were used to determine the positive signals and set compensation values to correct for

spectral overlap. The signal was normalized by running Quantum FITC and PE-Cy5 MESF beads (Bangs Laboratories, Inc., Fishers, IN).

To observe the fluorescence of polyplexes, the cells were seeded on 2-well microscope cover glass #1.5 at a concentration of 1×10^5 cells per well. After treatment with polyplexes according to the above procedure, the cells were fixed with 2% PFA and mounted with Prolong Gold (with DAPI). Fluorescence images were obtained using a confocal microscope (Olympus FV-500) employing a 60× oil immersion objective.

Three different lasers were used for the confocal images: the 405 nm line of a blue diode laser for DAPI stained nuclei, the 488 nm line of an argon ion laser for the AF488-labeled G5 or G7 dendrimers, and the 633 nm line of a HeNe laser for Cy5 labeled DNA or AF647 labeled CTB subunit. The internalization of polyplexes under the incubation conditions employed was confirmed by obtaining *z*-stack confocal images. These images demonstrated that the punctate distributions observed in the confocal images presented in this work primarily represent internalized polyplexes, not membrane adsorbed polyplexes.

Cell-Lysis Preparation and Protein-Concentration Determination. The six cell lines were seeded on 10 cm dishes at a cell density of 2×10^6 and cultured in complete medium until confluence. The cells were scraped off, and cell pellets were collected by centrifuge (RT, 210*g* for 5 min). A 300 μL lysis buffer (150 mM NaCl, 1% NP-40, 50 mM Tris, pH 8.0 and a tablet of cocktail of protease inhibitor) was added to the pellets, which were then placed on ice for at least half an hour with a discontinuous vortex. The supernatant of the cell lysates was collected by centrifuge at 4 °C, 450*g* for 5 min.

A BCA (bicinchoninic acid) assay was used to determine the total protein concentration of cell lysates. Briefly, protein assay reagent A was mixed with B (A/B = 50/1) to make the reaction solution. Next, 200 μL of reaction solution was added to 10 μL samples of cell lysates or standard BSA solution. The plate was incubated at 37 °C for 30 min. The absorption of samples was then determined at 562 nm, and the total protein concentration was calculated according to the standard BSA curve.

Detection of GM1 Expression by Dot Blot. For each sample, 10 μg of total protein in 2 μL of cell-lysis buffer was dotted on a strip of nitrocellulose membrane, with 2 μL of water as a negative control, and 7.5 ng of GM1 in 2 μL of water as a positive control. To make a GM1 standard dot blot, 2 μL GM1 solutions at differing amounts (from 7.5 pg to 30.7 ng) were dotted on the membrane. The membrane was blocked with 5% skim milk in TBST (10 mM Tris, 145.4 mM NaCl, 0.1% Tween-20, pH 8.0) for 1 h at room temperature (RT). The membrane was then incubated with CTB-HRP (200 ng/mL) for 1 h at RT, and HRP was detected by a chemiluminescent substrate kit. After this, the blots on the membrane were exposed to a film.

After being incubated with 80 μg/mL GM1 overnight, the cells were rinsed with PBS to remove non-cell-associated GM1, and cell-associated GM1 was detected, according to the above protocol.

Effect of GM1 on the Endocytosis of Polyplexes. The cells were seeded on 6-well plates at a concentration of 2×10^5 cells per well and incubated overnight with serum-free medium containing 80 μg/mL GM1. The non-cell-associated GM1 was removed by rinsing the cells with PBS.

According to the same procedure as described in the endocytosis of polyplexes, the cells were treated with G5 or G7 polyplexes. As a positive control, the cells were incubated with 1 μg/mL CTB-AF647 for 1 h. Parallel experiments of polyplexes and CTB were done on GM1 untreated cells according to the same endocytosis procedure. The fluorescence intensity of samples was determined by flow cytometry, and the images were taken under confocal microscope.

Effect of Ganglioside Inhibitor PPMP on the Endocytosis of Polyplexes. DL-Threo-1-phenyl-2-palmitoylamino-3-morpholino-1-propanol (PPMP), an inhibitor of glucosylceramide synthase, was used to block the synthesis of GM1. The 10 μM PPMP concentration used for these experiments was the highest concentration we could employ in these cell lines without inducing cytoxicity. Cos-7, 293A and HeLa cells, which have an initial GM1 expression, were seeded on 6-well plates at a concentration of 5×10^4 cells per well. The cells were grown in the presence of medium containing 10 μM PPMP and 5% serum at 37 °C for 3 days. After this, GM1 expression on the cells was detected by dot blot according to the protocol described before.

To estimate the influence of PPMP to endocytosis, the cells were treated with PPMP for 3 days, and then incubated with polyplexes according to the procedure of endocytosis of polyplexes. With CTB-AF647 (1 μg/mL) as a positive control, the fluorescence intensity of polyplexes in PPMP-treated cells was determined by flow cytometry and compared with that in PPMP-untreated cells from parallel experiments.

Infection of Cells with AdCAV-1. HeLa, KB, C6, Cos-7, and HepG2 cells were seeded on 6-well plates at a concentration of 5×10^4 cells per well, and infected by AdCAV-1(titer: 1×10^{10} pfu/mL) at MOI (multiplicity of infection) 10 or 30 in 500 μL of cell culture medium with 5% serum at 37 °C for 90 min. Into each well, 1 mL of complete medium was added, and the cells were incubated for 48 h so that the infected cells could express the caveolin-1 protein. To establish a control, parallel experiments were conducted using an empty adenovirus vector (Adnull, titer: 1×10^{10} pfu/mL) to infect the cells at the same dose of MOI to estimate the influence of adenovirus alone on the cells.

Detection of CAV-1 Expression by Western Blot. The cells were seeded on 6-well plates at a concentration of 5×10^4 cells per well, and were infected with AdCAV-1 (MOI 10 or 30) according to the procedure described in the section Infection of Cells with AdCAV-1. After 48 h, the cells were collected, and CAV-1 expression in cell lysates (in 5 μg of total protein) was determined by Western blot by using a first antibody of rabbit-anti-caveolin-1 polyclonal antibody (1:1000) and a second antibody of goat-anti-rabbit IgG-HRP

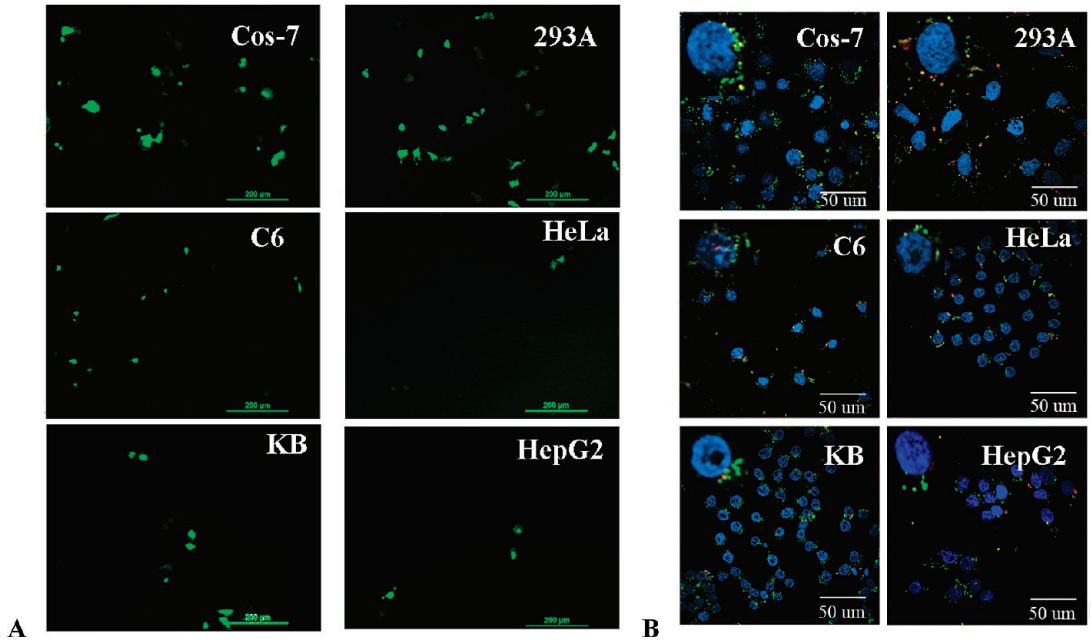

Figure 1. Gene expression after cells are transfected by G7 dendrimers (A) and fluorescence images of the internalized G7 polyplexes in different cell lines (B). (A) Images of GFP expression 48 h after transfection by G7 dendrimers at an *N*/*P* ratio of 10. (B) Confocal microscopy images of G7 polyplexes in different cell lines 6 h after transfection by G7 dendrimers at an *N*/*P* ratio of 10. Alexa Fluor 488 (AF488, green)-labeled G7 dendrimers and Cy5 (red)-labeled plasmid luciferase (Luc) were used to make polyplexes. Cell nuclei were stained by DAPI resulting in blue fluorescence in the images. Representative fluorescence image from a single cell is amplified and displayed at the top left corner of each image.

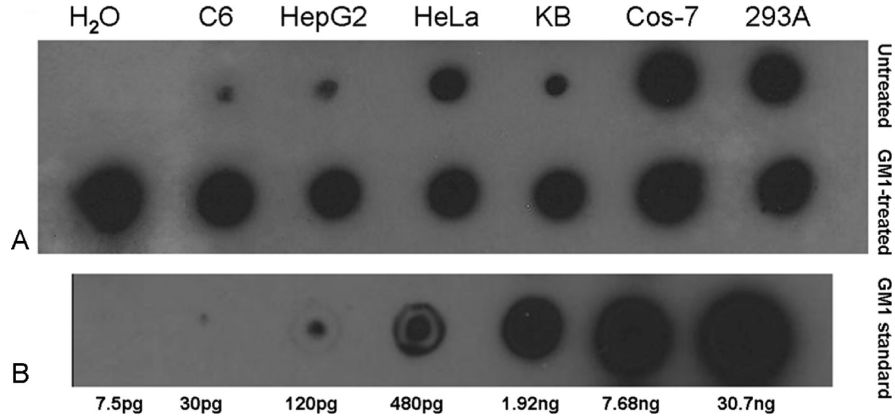

Figure 2. GM1 expression in different cell lines detected by dot blot. Each dot represents the amount of GM1 in 10 μg of total proteins from cell lysates. HRP-tagged cholera toxin B subunit (CTB) was used as a specific binding and detection reagent. (A) Top row, initial GM1 expression (from left to right): 2 μL of water (negative control); C6; HepG2; HeLa; KB; Cos-7; 293A. Bottom row, GM1 expression after cells were treated with cell culture medium containing 80 μg/mL GM1 overnight (from left to right): 7.5 ng of GM1 in 2 μL of water (positive control); C6; HepG2; HeLa; KB; Cos-7; 293A. (B) GM1 standard dot blot (from left to right): 7.5 pg; 30 pg; 120 pg; 480 pg; 1.92 ng; 7.68 ng; 30.7 ng.

(1:7500). The internal control was α-tubulin (1:10,000 dilution for the first antibody and 1:6000 dilution for the second antibody). The protein bands were presented using an HRP chemiluminescence substrate kit and exposed to a film.

CAV-1 Immunofluorescence Staining. The cells were seeded on 2-well chambers with a cell concentration of 1×10^5 per well and then grew overnight to attach to the surface of the wells. After being washed with PBS and fixed with 2% PFA, the cells were incubated with 0.5% Triton X-100 (in 1× PBS) at 37 °C for 15 min to expose the antigens, and was followed with 10% goat serum (in 1× PBS) for 30 min to block unspecific binding spots. The cells were incubated with a rabbit-anti-caveolin-1 polyclonal antibody (1:100) at 37 °C for 2 h and rinsed with PBS. The cells were then incubated with a TRITC-goat-anti-rabbit second antibody (1:200 diluted in PBS with 0.1% Triton X-100) at RT for 1 h, rinsed with PBS and mounted by Prolong Gold (with DAPI). Parallel experiments were done according to the same procedure, but the first antibody was replaced by the same volume of PBS with 0.5% Triton X-100 to verify the specificity of the staining. The stained monolayers of cells

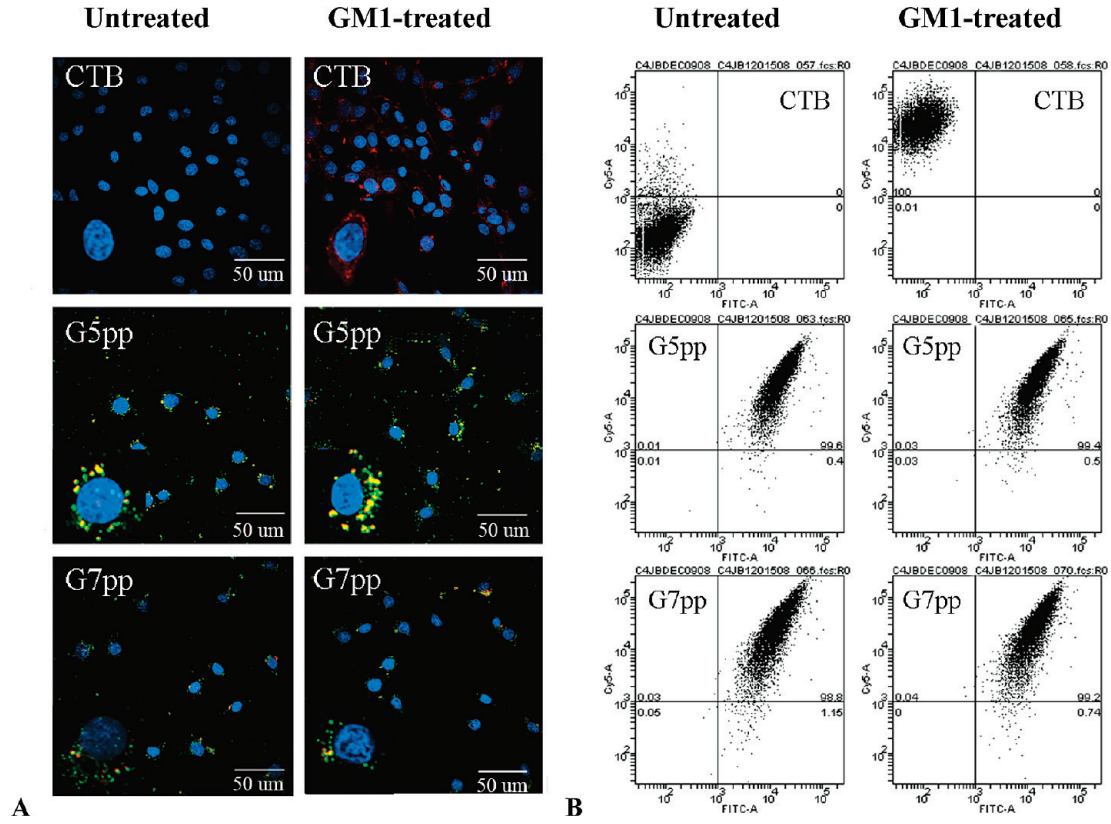

Figure 3. Confocal microscopy images (A) and flow cytometry graphs (B) of CTB (1 μg/mL), G5 polyplexes and G7 polyplexes in C6 cells before and after treatment of cells with GM1. Polyplexes were made by G5-AF488 or G7-AF488 with Cy5-labeled plasmid Luc at *N*/*P* ratio of 10. **A:** Confocal microscopy images of CTB, G5 polyplexes and G7 polyplexes in C6 cells before (left column) and after (right column) treatment of cells with 80 μg/mL GM1 overnight. The results indicated that the internalization of the positive control, AF-647-labeled CTB (red), is significantly increased after supplementation of GM1 to the membrane of C6 cells, but has no influence on the endocytosis of G5 and G7 polyplexes. A representative fluorescence image from a single cell is amplified and displayed at the bottom left corner of each image. *Z*-Scans were performed to confirm that the CTB was internalized into the cell. (B) Flow cytometry graphs of CTB, G5 polyplexes and G7 polyplexes in C6 cells before (left column) and after (right column) treatment of cells with 80 μg/mL GM1 overnight. The results illustrated that the cell population of CTB shifts significantly to the increase of fluorescence intensity after supplementation of GM1 to the membrane of C6 cells. However, the fluorescence intensity of the cell population, which were transfected with G5 and G7 polyplexes, was not changed obviously before and after treatment of C6 cells with GM1.

were observed and fluorescence images were taken using confocal microscopy.

Effect of CAV-1 on the Endocytosis of Polyplexes. The cells were seeded and infected by AdCAV-1 (MOI 30) for 48 h, then they were incubated with the polyplexes of G5-AF488 or G7-AF488 and plasmid Luc-Cy5 according to the endocytosis of polyplexes procedure. With CTB-AF647 (1 μg/mL) as a positive control, the cell-associated fluorescence intensity of polyplexes was analyzed by flow cytometry. The results were compared with those from adenovirus untreated cells or adenovirus vector only (Adnull) treated cells according to the same endocytosis procedure.

Double Upregulation of CAV-1 and GM1. To study the influence of double upregulation of CAV-1 and GM1 to the endocytosis of polyplexes in the caveolin-1 and GM1 double deficient cell lines (HepG2, KB and HeLa cells), the cells were first infected by AdCAV-1 or Adnull (MOI 30) for 48 h, and then incubated with 80 μg/mL GM1 overnight. After this, the cells were incubated with G7 polyplexes or CTB according to the procedure for the endocytosis of polyplexes, and results were compared with those from the adenovirus and GM1 untreated cells. The fluorescence images of polyplexes or CTB were taken under confocal microscope.

Results

Transfection and Endocytosis of G7 Polyplexes. As shown in Figure 1 (panel A), the fluorescence of GFP was observed for all six cell lines 48 h after transfection. However, many more Cos-7 and 293A cells expressed GFP (~5%) as compared to the C6, HeLa, KB, or HepG2 cell lines (1−3%). The C6, HeLa, Cos-7, and 293A cell lines all showed greater than 90% polyplex uptake whereas the HepG2 and KB cell lines exhibited 60 and 72%, respectively.

GM1 Expression in Different Cell Lines. The specificity of a dot blot is shown on the left line in Figure 2A. The dot from 2 μL of water as a negative control did not form a blot. The positive control consisting of 7.5 ng of GM1 formed

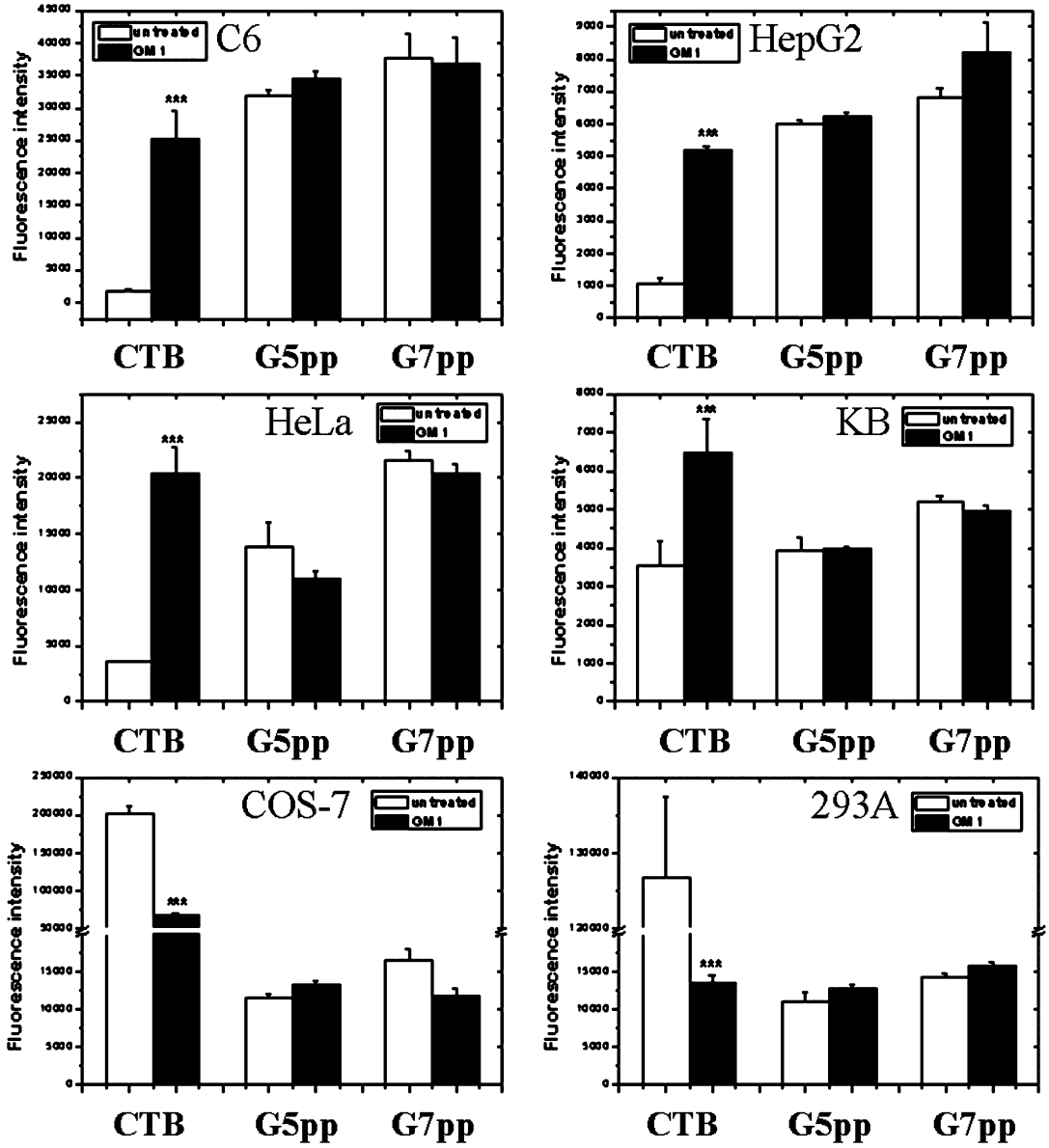

Figure 4. Fluorescence intensity of CTB (-AF647) and polyplexes (Cy5-labeled plasmid Luc) from C6, HepG2, HeLa, KB, Cos-7 and 293A cells before (white column) and after (black column) treatment of cells with GM1 (80 μg/mL) measured by flow cytometer. The percentage of the positive cell population for each sample is shown in Table S1 in the Supporting Information.

a neat blot on the membrane. The results also indicated that, among all of the six cell lines, Cos-7 and 293A cells have much more initial GM1 expression. In terms of the expression of GM1 in the other four cell lines, HeLa cells have less than 293A cells, there are fewer GM1 in the KB cells than in the HeLa cells, and the HepG2 and C6 cells have almost none.

After the cells were incubated with 80 μg/mL GM1 overnight (the second row in Figure 2A), cell-associated GM1 in the cell lysates of the six cell lines had increased to greater than or equal to normal cell levels. The GM1 standard dot blot (Figure 2B) illustrates that the blot size of GM1 is correlated with the GM1 concentration in the solution. Therefore, the GM1 content in the cell lysates before and after treatment with GM1 can be estimated.

Effect of GM1 on the Endocytosis of Polyplexes. The influence of supplemented GM1 in the cell membrane to the endocytosis of polyplexes is illustrated in Figures 3 and 4. After being presented with the exogenous GM1 in the C6 cell membrane, the fluorescence of internalized CTB-AF6, a positive control, increased by a factor of 14 ($P < 0.001$) compared with that of untreated cells (Figure 3, panel A). The cell population also exhibited a shift to greater fluorescence intensity (Figure 3, panel B). However, the fluorescence of internalized G5 polyplexes and G7 polyplexes did not change with the addition of GM1 (Figure 3).

Similar results were obtained for three other GM1-deficient cell lines: HepG2, HeLa and KB cells (Figure 4). Supplementation with GM1 increased the internalization of CTB by 4.9- ($P < 0.001$), 5.7- ($P < 0.001$), and 1.8- ($P < 0.001$)

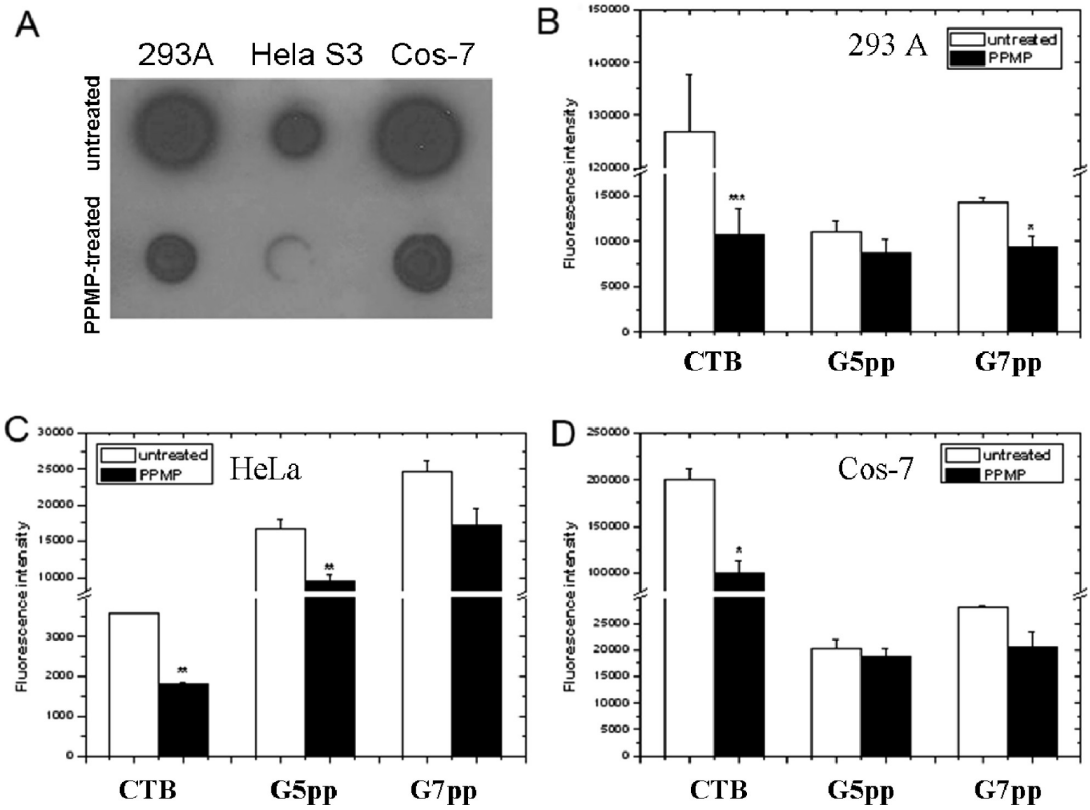

Figure 5. Effect of ganglioside inhibitor, PPMP, to the endocytosis of CTB and polyplexes. (A) GM1 expression before (top row) and after (bottom row) treatment of 293A (left), HeLa (middle) and Cos-7 (right) cells with cell culture medium containing 10 μM PPMP for 3 days measured by dot blot. Fluorescence intensity of CTB (-AF647) and polyplexes (Cy5-labeled plasmid Luc) from 293A (B), HeLa (C) and Cos-7 (D) cells before (white column) and after (black column) treatment of cells with 10 μM PPMP measured by flow cytometer.

fold in HepG2, HeLa, and KB cells versus untreated cells, respectively. However, the internalization of G5 polyplexes and G7 polyplexes was not influenced by supplementation with GM1 in these three cell lines ($P > 0.01$).

The internalization of G5 and G7 polyplexes was also not notably changed after the addition of GM1 to the two GM1-sufficient cell lines, Cos-7 and 293A (Figure 4), whereas the fluorescence intensity of the positive control, CTB-AF647, was significantly reduced 66% ($P < 0.001$) in Cos-7 cells and 89% ($P < 0.001$) in 293A cells after the addition of the extra GM1.

Effect of Ganglioside Inhibitor PPMP on the Endocytosis of Polyplexes. As shown in Figure 5A, after 293A, HeLa and Cos-7 cells were treated with 10 μM PPMP for 3 days, the GM1 content dramatically decreased in all of these three naturally GM1-expressing cell lines. After the reduction of the GM1 expression by a ganglioside-synthesis inhibitor, PPMP, the internalization of the positive control CTB-AF647 was markedly decreased 92% ($P < 0.001$), 50% ($P < 0.005$), and 51% ($P < 0.01$) in 293A, HeLa and Cos-7 cells, respectively. However, the endocytosis of G5 and G7 polyplexes was inconsistently influenced by this general ganglioside inhibitor. Among all of the three cell lines, the fluorescence intensity of G7 polyplexes was reduced 34% ($P < 0.01$) only in 293A cells, but the fluorescence of G5 polyplexes in the same 293A cells displayed no statistical difference before and after (20% reduction, $P > 0.01$) treating the cells with PPMP (Figure 5B). Similarly inconsistent results were obtained for HeLa cells (Figure 5C, the fluorescence of G5 and G7 polyplexes reduced 44% ($P < 0.005$) and 30% ($P > 0.01$), respectively). In Cos-7 cells, the internalization of G5 and G7 polyplexes was not significantly influenced by PPMP by 8% ($P > 0.01$) and 27% ($P > 0.01$) decrease of fluorescence respectively after the cells being treated by PPMP.

Detection of CAV-1 Expression. CAV-1 expression was detected by Western blot (Figure 6, part I) and immunofluorescence staining (Figure 6, part II). With α-tubulin as an internal control (Figure 6, part I, A) in Western blot, the initial CAV-1 expression in the five cell lines revealed that C6 cells had the most CAV-1 expression whereas HepG2 cells had almost no CAV-1 expression (Figure 6, part I, C). The expression level of CAV-1 in Cos-7, HeLa and KB cells occurred midway between C6 and HepG2 cells and in a decreasing amount (Figure 6, part I, B and C). After the HeLa and KB cells were infected with AdCAV-1 at two different doses (MOI 10 and 30) for 48 h, the protein expression of CAV-1 consistently increased in a dose-dependent manner (Figure 6, part I, B). Similar results were observed for Cos-7

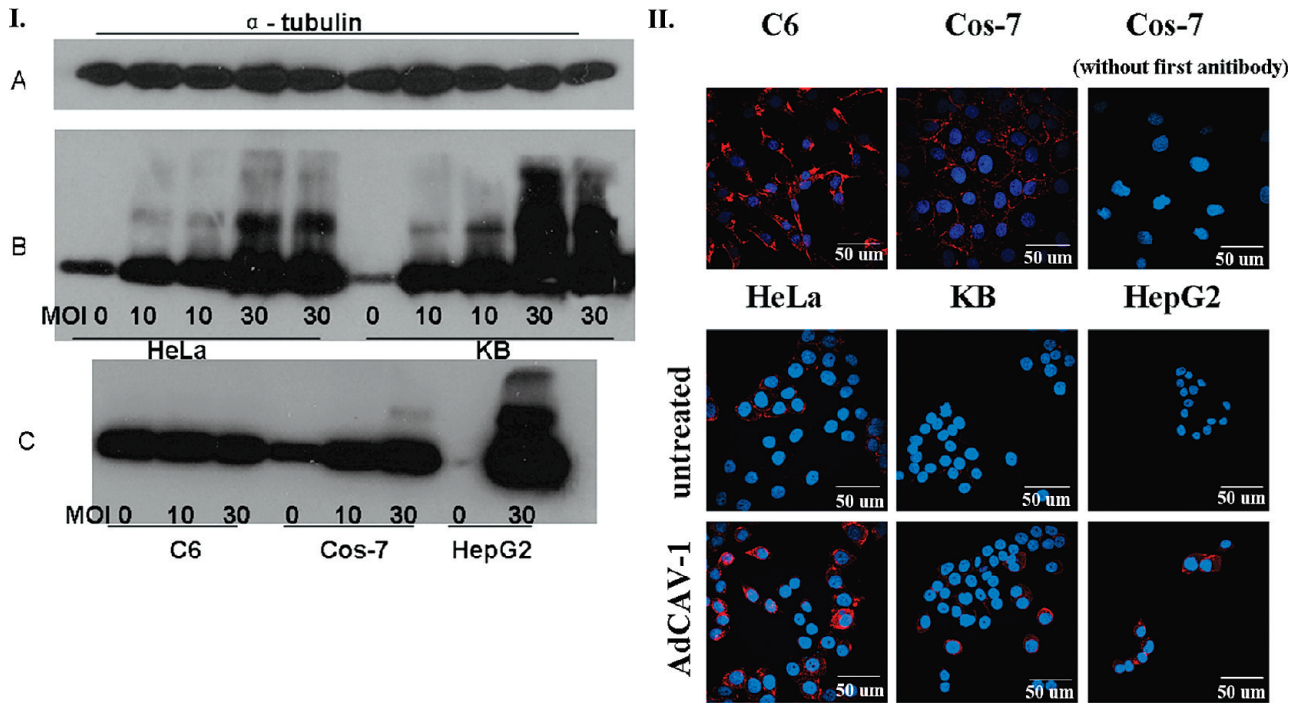

Figure 6. Cav-1 expression in different cell lines measured by Western blot (part I) and immunofluorescent staining (part II). Part I: Aimed protein expression from 5 μg of total protein of cell lysates determined by Western blot. (A) The protein expression of internal-control α-tubulin with mouse anti-α-tubulin as the primary antibody, and HRP-tagged goat anti-mouse IgG as the secondary antibody. (B) Cav-1 expression (from left to right): HeLa (initial); AdCAV-1 infected HeLa at MOI 10; MOI 10 parallel-infected HeLa; AdCAV-1 infected HeLa at MOI 30; MOI 30 parallel-infected HeLa; KB (initial); AdCAV-1 infected KB at MOI 10; MOI 10 parallel-infected KB; AdCAV-1 infected KB at MOI 30; MOI 30 parallel-infected KB. (C) Cav-1 expression (from left to right): C6 (initial); AdCAV-1 infected C6 at MOI 10; AdCAV-1 infected C6 at MOI 30; Cos-7 (initial); AdCAV-1 infected Cos-7 at MOI 10; AdCAV-1 infected Cos-7 at MOI 30; HepG2 (initial); AdCAV-1 infected HepG2 at MOI 30. In B and C, rabbit anti-CAV-1 and HRP-tagged goat anti-rabbit IgG were used as the primary and the secondary antibodies, respectively. Part II: Cav-1 expression in different cell lines determined by immunofluorescent staining using rabbit anti-CAV-1 as the primary antibody, and TRITC-tagged goat anti-rabbit IgG (red fluorescence) as the secondary antibody. Top row: initial CAV-1 expression in C6 (left) and Cos-7 (middle) cells, detection of CAV-1 in Cos-7 without the primary antibody (right). Middle row: initial CAV-1 expression in HeLa (left), KB (middle) and HepG2 (right) cells. Bottom row: CAV-1 expression in HeLa (left), KB (middle) and HepG2 (right) after infecting cells with AdCAV-1 at MOI 30. Note that the initial CAV-1 expression-level in these cell lines is C6 > Cos-7 (normal) > HeLa > KB > HepG2 (almost none). After infecting cells with AdCAV-1, the protein expression of CAV-1 is successfully upregulated in most of the cell lines except for C6 cells, and the infection efficacy is consistent within the same dose of adenovirus.

and HepG2 cells (Figure 6, part I, C), but the CAV-1 expression was not upregulated by AdCAV-1 in C6 cells even at the high dose of MOI 30 (perhaps because the initial CAV-1 expression is abundant in C6 cells).

Figure 6, part II, illustrates the results of immunofluorescence staining for CAV-1 protein. The specificity of staining is demonstrated by the top-right image. Immunofluorescence staining of the CAV-1 protein in Cos-7 cells without the primary antibody, but with a TRITC-tagged secondary antibody, resulted in no red fluorescence from nonspecific staining. The amount of initial CAV-1 protein in the five cell lines (first and second rows in Figure 6, part II) follows the same trend as the results from Western blot. After the HeLa, KB and HepG2 cells were infected with AdCAV-1 at MOI 30 for 48 h, the increase of red fluorescence around the cell membrane and inside the cells after staining indicated the increase of CAV-1 protein expressed by AdCAV-1 in the three cell lines (third row in Figure 6, part II).

Effect of CAV-1 on the Endocytosis of Polyplexes. As shown in Figure 7, compared with that of Adnull infected cells, the fluorescence intensity of G5 and G7 polyplexes did not significantly change ($P > 0.01$) after the cells were infected by AdCAV-1 at MOI 30 in all HeLa, HepG2, KB and Cos-7 cells. In these cells the CAV-1 protein was clearly upregulated by AdCAV-1 at the same dose of MOI 30 according to the results of Western blot. The endocytosis of polyplexes can be influenced by empty adenovirus vector itself, since the fluorescence intensity of G5 and G7

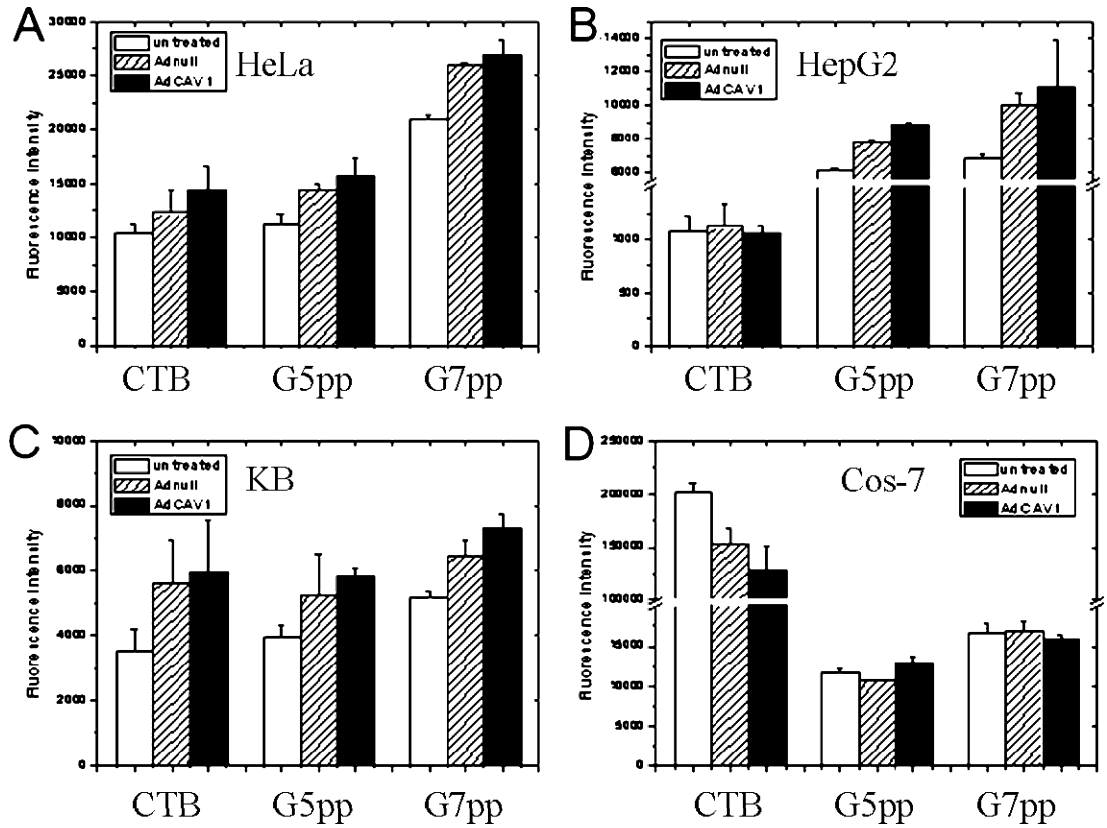

Figure 7. Fluorescence intensity of CTB (-AF647) and polyplexes (Cy5-labeled plasmid Luc) before (white column) and after (black column) upregulation of CAV-1 by AdCAV-1 in HeLa (A), HepG2 (B), KB (C) and Cos-7 (D) cells measured by flow cytometer, with the same dose (MOI 30) of empty adenovirus vector (Adnull)-infected cells as the control (hatched column). Note that upregulation of the protein expression of CAV-1 does not increase the endocytosis of G5 and G7 polyplexes in all of the four cell lines after excluding the influence of the adenovirus vector ($P > 0.01$).

polyplexes was increased to some extent in Adnull only infected HeLa, HepG2 and KB cells.

Upregulation of the CAV-1 protein in Cos-7 cells, a CAV-1 and GM1-sufficient cell line, did not contribute to an increase of the internalization of CTB (Figure 7A). The internalization of CTB was also not increased after upregulation of CAV-1 protein by AdCAV-1 in the HeLa, HepG2 and KB cell lines (Figure 7A−C, $P > 0.01$; Figure 8, part I, middle line). However, CTB internalization was significantly increased by double upregulation of CAV-1 and GM1 for the HeLa ($P < 0.005$), KB ($P < 0.005$), and HepG2 ($P < 0.001$) cell lines which are both GM1-and CAV-1-deficient (Figure 8, part I, right line). Note that the increase in internalization persisted even after controlling for the influence of adenovirus vector (Figure 8, part II, A). However, at the same condition, the fluorescence intensity of G7 polyplexes was not increased by double upregulation of CAV-1 and GM1 in these three cell lines (Figure 8, part II, B, $P > 0.01$). Note that an apparent increase in internalization is in fact an artifact of the adenovirus vector treatment.

Discussion

Evidence for Lipid Raft Mediated Endocytosis: The Role of GM1. Literature evidence for the LRME pathway for cationic polymer/DNA polyplexes was primarily provided by colocalization with CTB and CAV-1 dependence on protein expression.[12,13] We readily reproduced the literature data for colocalization with CTB (see Figure S1 in the Supporting Information). However, we were concerned about the possibility of interaction between CTB and the polyplexes prior to interacting with the cells. If this occurred, then colocalization with CTB would not prove a GM1 interaction. Initial studies examining the endocytosis mechanism for G7 PAMAM dendrimer raised substantial concerns when we determined that the polymer itself did interact with CTB external to the cell and that this caused the colocalization. Indeed, the polymer by itself exhibited no GM1 dependence for internalization into cells.[26] However, since endocytosis mechanisms are highly size dependent,[28−30] the data obtained for the polymer alone was not conclusive regarding polyplex behavior.

Experiments exploring the level of GM1 expression (Figure 2) as a function of GFP expression in the Cos-7, 293A, C6,

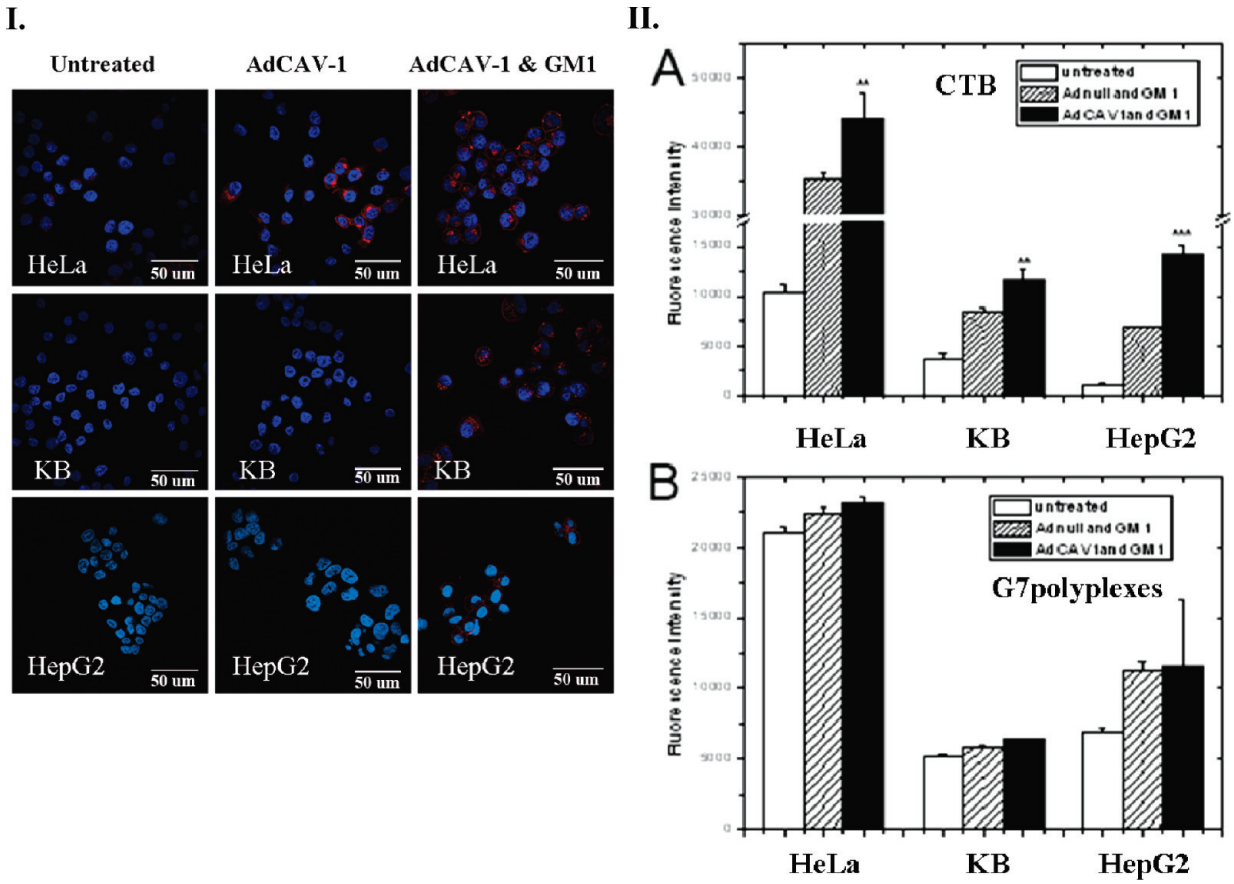

Figure 8. Effect of double upregulation of CAV-1 and GM1 on the endocytosis of CTB and polyplexes in CAV-1- and GM1-deficient cell lines (HeLa, KB and HepG2 cells). Part I: Confocal microscopy images of CTB (-AF647) before (left) and after single upregulation of CAV-1 (middle) and double upregulation of CAV-1 and GM1 (right) in HeLa (top row), KB (middle row) and HepG2 (bottom row) cells. Note that the internalization of CTB is significantly increased after double upregulation of CAV-1 and GM1 in all of the three cell lines, but single upregulation of CAV-1 has no dramatic influence on the endocytosis of CTB. Part II: Fluorescence intensity of CTB (A) and G7 polyplexes (B) before (white column) and after (black column) double upregulation of CAV-1 and GM1 in HeLa, KB and HepG2 cells measured by flow cytometer, with the same dose of Adnull- and GM1-treated cells as control (hatched column). Note that compared with Adnull- and GM1-treated cells, the internalization of CTB in CAV-1 and GM1 double-treated cells is significantly increased in all of the three cell lines (*** $P < 0.001$, ** $P < 0.005$). However, double upregulation of CAV-1 and GM1 has no significant influence on the endocytosis of G7 polyplexes ($P > 0.01$).

HeLa, KB, and HepG2 cell lines (Figure 1) demonstrated that the two cell lines (Cos-7 and 293A) with the most GM1 did indeed express the most GFP. However, the C6 cell line, which contains little to no GM1, still internalized both the G5 and G7 PAMAM polyplexes and GFP was expressed. By way of contrast, CTB did not internalize into C6 cells unless they had been preincubated with exogenous GM1 (Figure 3). An additional comment about the GM1 dot blot studies is in order. Although C6 cells should have no GM1 blot, we still detected a trail which is attributed to other gangliosides. This is attributed to a small degree of nonspecificity of the CTB-HRP binding reagent which can also bind to some extent with other gangliosides in the cell lysates and form a tiny blot on the membrane.[38,39]

Further evidence that the polyplexes do not follow a GM1 internalization pathway is provided by experiments in which Cos-7 and 293A cells, which contain substantial GM1 in the plasma membrane, were incubated with additional exogenous GM1 resulting in a 66% ($P < 0.001$) and 89% ($P < 0.001$) reduction in internalization of CTB, respectively. Model studies suggest that some of the extra GM1 added to the GM1-sufficient cell lines may not be able to insert into the cell membrane and instead form clusters outside the cells which will compete with natural GM1 to bind with CTB.[40] The binding of CTB with the outside GM1 cluster will decrease

(38) Chinnapen, D. J. F.; Chinnapen, H.; Saslowsky, D.; Lencer, W. I. Rafting with cholera toxin: endocytosis and trafficking from plasma membrane to ER. *FEMS Microbiol. Lett.* **2007**, *266*, 129–137.

(39) Kuziemko, G. M.; Stroh, M.; Stevens, R. C. Cholera toxin binding affinity and specificity for gangliosides determined by surface plasmon resonance. *Biochemistry* **1996**, *35*, 6375–6384.

(40) Shi, J. J.; Yang, T. L.; Kataoka, S.; Zhang, Y. J.; Diaz, A. J.; Cremer, P. S. GM(1) clustering inhibits cholera toxin binding in supported phospholipid membranes. *J. Am. Chem. Soc.* **2007**, *129*, 5954–5961.

the internalization of CTB. It is believed that CTB must simultaneously bind with five outside neighboring glucose residues of transmembrane GM1 before being internalized inside the cytosome of the cells.[41] The polyplex behavior again contrasts with that of CTB and shows no change in internalization upon the addition of GM1 to these two cell lines.

The role of GM1 was also explored by treating the 293A, HeLa, and Cos-7 cells with ganglioside inhibitor PPMP which substantially decreased GM1 content in all three cell lines (Figure 5A). CTB internalization decreased by 92% ($P < 0.001$), 50% ($P < 0.005$), and 51% ($P < 0.01$), respectively (Figure 5B−D), consistent with a GM1 dependent internalization process. By way of contrast, the G5 and G7 PAMAM polyplexes exhibited less of a dependence or none at all. In light of the well-behaved uptake studies illustrated in Figures 3 and 4 and the well-behaved nature of the CTB with the PPMP inhibitor, we ascribe the cell-line dependent PPMP effect seen for the polyplexes as resulting from nonspecific inhibition effects off of the GM1 pathway. Problems of nonspecificity for endocytic inhibitors are common and were the subject of a recent detailed review.[42]

Evidence for Lipid Raft Mediated Endocytosis: The Role of CAV-1. The other major evidence for a LRME endocytosis pathway for PAMAM dendrimer polyplexes was the observed dependence on CAV-1.[13] In order to explore this aspect of the pathway, a set of cells were selected containing a variety of CAV-1 expression as illustrated by Western blot and immunofluorescence staining (Figure 6). The studies confirmed that HepG2 contained little CAV-1[43,44] yet still shows substantial uptake and expression of PAMAM polyplexes (Figures 1 and 4). Considering all of the cell lines employed, despite substantial differences in the level of CAV-1 expression, no systematic change in polyplex behavior was observed. To further explore the role of CAV-1, the HeLa, HepG2, KB, and Cos-7 cell lines were upregulated by infection with AdCAV-1.[45] Although increases in the level of polyplex uptake were observed, consistent with previous reports for HeLa and HepG2,[13] the increases were found to be identical to the changes induced by treating the cells with the empty adenovirus vector. In other words, the upregulation of CAV-1 did not increase uptake beyond that of Adnull infected cells (Figure 7).

As a final comparison, the HeLa, KB, and HepG2 cell lines, which are both GM1 and CAV-1 deficient, were employed to examine the effect of double upregulation of GM1 and CAV-1 on both CTB and PAMAM polyplex internalization. Once again, the CTB exhibited an increase in internalization as expected for a GM1/CAV-1 LRME internalization mechanism. By way of contrast, the G7 PAMAM polyplexes showed no increased internalization.

Developing Perspectives on Endocytosis Pathways. As noted in the introduction, the mechanism(s) of cellular internalization for both cationic dendrimers[19−26] and cationic polyplexes have been intensely studied.[9−18] In previous studies we had demonstrated that the GM1/CAV-1 pathway was not followed for G7 dendrimers.[26] In this study, we show that G5- and G7-based polyplexes also do not follow the GM1/CAV-1 pathway. The understanding of the pathways of internalization of polymers and polymer/DNA polyplexes remains a major challenge for developing widely effective transfection agents capable of efficient expression. As noted in recent reviews, the detailed mechanisms remain poorly understood and are likely more complex than relatively simple catagories used to date.[46−48]

Summary

The GM1/CAV-1 LRME mechanisms for the endocytosis of G5 and G7 PAMAM polyplexes were tested for the Cos-7, 293A, C6, HeLa, KB, and HepG2 cell lines. Cholera toxin subunit B (CTB) was employed as a positive control. These studies show that the GM1/CAV-1 LRME mechanism is not followed for the G5 and G7 PAMAM polyplexes in these cell lines. Other potential endocytosis pathways are currently under exploration.

Acknowledgment. This project was supported by federal funds from the National Institute of Biomedical Imaging and Bioengineering (R01-EB005028) and by the fellowship for R.Q. by the National Natural Science Foundation of China (No. 30500197 and No. 30971241).

Supporting Information Available: Confocal fluorescence images of CTB colocalization with polyplexes in Cos-7 cells (Figure S1), confocal fluorescence and brightfield images of GFP expression in Cos-7 cells using G7 dendrimers (Figure S2), and a table of the positive uptake cell populations for CTB, G5 polyplexes, and G7 polyplexes in C6, HepG2, HeLa, KB, Cos-7, and 293A cell lines. This material is available free of charge via the Internet at http://pubs.acs.org.

MP900241T

(41) Merritt, E. A.; Sarfaty, S.; Vandenakker, F.; Lhoir, C.; Martial, J. A.; Hol, W. G. J. Crystal-Structure of Cholera-Toxin B-Pentamer Bound to Receptor G(M1) Pentasaccharide. *Protein Sci.* **1994**, *3*, 166–175.

(42) Ivanov, A. I. *Pharmcological Inhibition of Endocytic Pathways: Is It Specific Enough to Be Useful*; Humana Press: Totowa, NJ, 2008; Vol. 440, pp 15−33.

(43) Rhainds, D.; Bourgeois, P.; Bourret, G.; Huard, K.; Falstrault, L.; Brissette, L. Localization and regulation of SR-BI in membrane rafts of HepG2 cells. *J. Cell Sci.* **2004**, *117*, 3095–3105.

(44) Pohl, J.; Ring, A.; Stremmel, W. Uptake of long-chain fatty acids in HepG2 cells involves caveolae: analysis of a novel pathway. *J. Lipid Res.* **2002**, *43*, 1390–1399.

(45) Frank, P. G.; Pedraza, A.; Cohen, D. E.; Lisanti, M. P. Adenovirus-mediated expression of caveolin-1 in mouse liver increases plasma high-density lipoprotein levels. *Biochemistry* **2001**, *40*, 10892–10900.

(46) Won, Y. Y.; Sharma, R.; Konieczny, S. F. Missing pieces in understanding the intracellular trafficking of polycation/DNA complexes. *J. Controlled Release* **2009**, *139*, 88–93.

(47) Midoux, P.; Breuzard, G.; Gomez, J. P.; Pichon, C. Polymer-Based Gene Delivery: A Current Review on the Uptake and Intracellular Trafficking of Polyplexes. *Curr. Gene Ther.* **2008**, *8*, 335–352.

(48) Conner, S. D.; Schmid, S. L. Regulated portals of entry into the cell. *Nature* **2003**, *422*, 37–44.